

# Standardizing Skullremodeling Surgery and Electrode Array Layout to Improve Tumor Treating Fields Using Computational Head Modeling and Finite Element Methods



N. Mikic, F. Cao, F. L. Hansen, A. M. Jakobsen, A. Thielscher,  
and A. R. Korshøj

## 1 Introduction

Tumor Treating Fields is a well-established treatment modality for glioblastoma (GBM) [1]. One factor that influences the efficacy of TTFields therapy is the electric field strength. High electric field intensities reduce the rate of tumor cell division *in vitro* [2] and increase progression-free survival (PFS) and overall survival (OS) in GBM patients, thus demonstrating the TTFields therapy dose-response relationship [3].

---

N. Mikic and F. Cao contributed equally with all other contributors.

---

N. Mikic (✉) · A. R. Korshøj  
Aarhus University Hospital, Department of Neurosurgery, Aarhus, Denmark

Aarhus University, Department of Clinical Medicine, Aarhus, Denmark  
e-mail: [nikmik@rm.dk](mailto:nikmik@rm.dk)

F. Cao · A. Thielscher  
Technical University of Denmark, Center for Magnetic Resonance, Department of Health Technology, Lyngby, Denmark

Danish Research Centre for Magnetic Resonance, Centre for Functional and Diagnostic Imaging and Research, Copenhagen University Hospital Amager and Hvidovre, Hvidovre, Denmark

F. L. Hansen  
Aarhus University Hospital, Department of Neurosurgery, Aarhus, Denmark

A. M. Jakobsen  
Aarhus University Hospital, Department of 3D Printing, Aarhus, Denmark

Korshøj et al. proposed in 2016 a novel surgical technique “skull-remodeling surgery” (SR-surgery) to increase the TTFields intensity. SR-surgery involves removing bone from the skull in the form of craniectomy, burrholes, or skull thinning. The hypothesis is by removing parts of the cranium, the resistance created by the bone is reduced and the electric field intensity is strengthened focally in the underlying tissue. By using realistic computational head models and finite element method it was concluded that SR-surgery could potentially increase the TTFields intensity by 60–70% in superficial tumors. Furthermore, it was concluded that several small burrholes would induce a greater increase in field strength than one large craniectomy per skull defect area, which is an important clinical safety consideration [4]. Computational studies also indicated that TTFields electrode array placement could be optimized when taking SR-surgery into account [5].

Feasibility of the SR-surgery concept was recently demonstrated in a small investigator-initiated, single-center, open-label phase 1 trial (OptimalTTF-1) from 2016 to 2019 with 15 first recurrent glioblastoma patients. For ethical- and risk-to-reward reasons one of the inclusion criteria was that the SR-surgery should increase the TTFields intensity by a minimum of 25%. This was validated using computational methods on patient-specific models. The median relative increase in the field intensity was 32% (range 25;59). The trial concluded that SR-surgery was safe without additional toxicity [6].

Subsequently, a randomized, comparative, multi-center, investigator-initiated interventional phase 2 trial (OptimalTTF-2) was launched in October 2020 [7]. The trial will include 84 first recurrence GBM patients randomized 1:1 to TTFields therapy with or without SR-surgery. All patients will receive physician’s choice medical oncological therapy. The primary endpoint is overall survival.

To simplify and standardize the intervention, the SR-surgery procedure is conducted using a standardizing operating procedure (SOP) that is easy to understand and replicate with minimum required training.

The specifications of the SOP are given below, and the following work shows preliminary documentation for the approach.

## 2 Method

### 2.1 Standardizing the SR-Surgery Configuration

A five burrhole SR-surgery configuration was chosen as shown in Fig. 1, based on previous research indicating higher efficacy compared to complete craniectomy [4]. The general rationale behind this configuration was to induce significant field enhancement in the peritumor and tumor region without compromising patient safety and with no requirement for protective headgear.

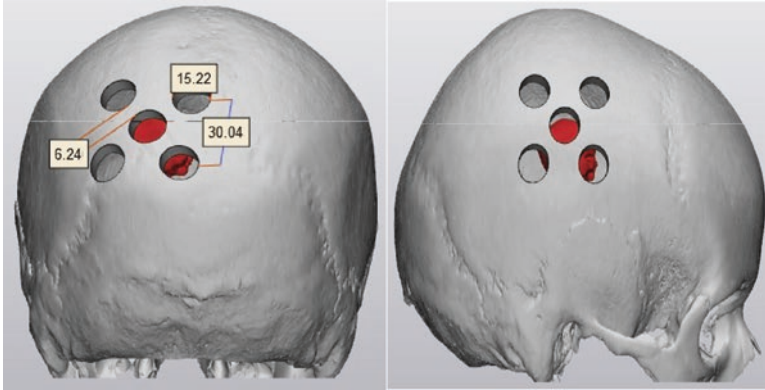


**Fig. 1** Five burrholes each 15 mm in diameter. Central burrhole placed above the tumor (marked in red)

**Suggested clinical procedure:**

1. Five burrholes are created each 15 mm in size.
2. The central burrhole should be placed directly above the tumor resection cavity or tumor remanent.
3. Electrodes are placed so that edge electrodes from one array in a pair are located above the holes or very close to the holes. The other array in the pair should be placed directly opposite on the other side of the head. Preferably, a direct line between the transducer located above the burr-holes and the central transducer on the opposite array in the pair should pass through the region of interest, i.e., the residual tumor or a region of the resection cavity with a predicted high risk of recurrence. This configuration should be achieved from both TTFields pairs.

## 2.2 *Technical Aspects of the SR-Surgery*

To support the neurosurgeons in implementing the procedure outline above and to ensure uniformity across the phase II trial centers, 3D printed, and sterilized templates were made to guide the neurosurgeons during surgery. Four templates with different radius curvatures (0.0, 3.2, 6.4, and 9.6 mm) were included in each sterilized pack to improve fitting in different areas of the skull (Figs. 2 and 3).

The neurosurgeon will decide perioperatively, after completion of the tumor removal where the bulk of the resection cavity or tumor remanent lies and place the central burrhole directly on top. If no residual tumor is left, the surgeon would place the central burrhole above the resection cavity or a part of the surrounding brain tissue where future recurrence is expectedly likely to occur. Placement of the burr-holes does not need to be restricted to the craniotomy existing bone plate used to access the tumor during resection. The template is placed as described above and

**Fig. 2** The four 3D printed templates are shown in a sterilized peel-pack. Each template curves slightly more than the next

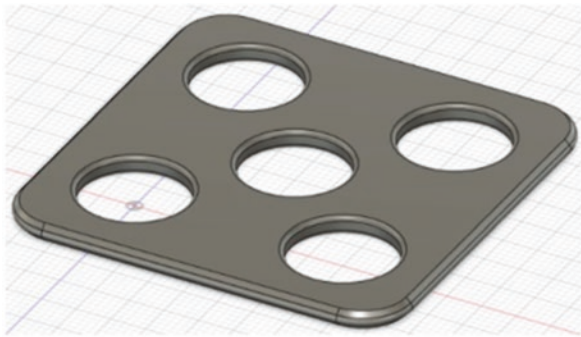


**Fig. 3** The concept and schematic of a 3D printed template

the five burrholes are marked with a high-speed electrical drill. The template is then removed during drilling and repeatedly repositioned until the right configuration is achieved. The additional procedure time is approximately 5–10 min, with minimal risk of dural- and cortical damage. Two examples are given in Figs. 4 and 5.

### ***2.3 Validating the SR-Surgery Configuration via Simulations***

To validate this SR-surgery configuration we used simulations of the electric fields generated by the TTFields therapy using a detailed head model constructed from structural MR images and the Finite-Element Method (FEM). The head model was initially created from a dataset of a healthy participant which was then adapted to emulate a trial patient's pathology based on their postoperative MRI and CT of the head.

**Fig. 4** A post-operative CT of the skull in a patient that underwent SR-surgery. In this case, the bone flap was big enough to fit all five burrholes while simultaneously having the central burrhole right above the resection cavity

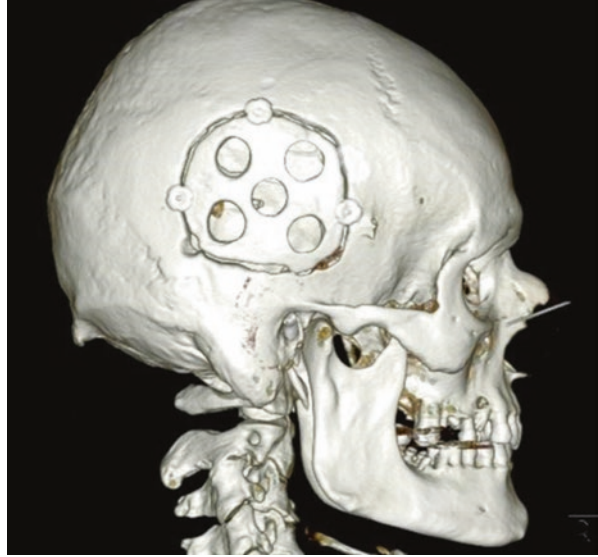


**Fig. 5** Perioperative photo. It shows a bone flap that is big enough to fit all five burrholes, however, the entire configuration was moved so that the central burrhole was over the bulk of the resection cavity. Therefore a “half burrhole” was created on the bone flap and the other half on the skull



More specifically, we created the computational head model using the example dataset “Ernie” in the SimNIBS software package as a proof-of-concept demonstration. The “Ernie” dataset corresponds to a young and healthy subject, including a high-resolution T1 and a T2 weighted image. Details on the “Ernie” dataset can be found in the documentation from the SimNIBS toolbox.

In our first step, an automated tissue segmentation was performed on the T1 and T2 weighted images of the “Ernie” dataset. The initial segmentation includes the following eight tissue compartments: white matter, gray matter, CSF, scalp, skull, muscle, blood, and eyeballs.

In our second step, the segmented image was visually inspected, and the configurations of the virtual tumor resection cavity, the residual tumor, and the burrholes were set manually based on the trial patient's postoperative MRI and CT of the head and were as follows:

1. A virtual sphere-shaped tumor resection cavity with a 2.5 cm diameter in the "Ernie" head model (Fig. 6a).
2. A cylinder-shaped funnel on the top of the tumor resection cavity mimics the surgical entry to the tumor. The funnel track has a 0.8 cm diameter.
3. A sphere-shaped tumor remanent of a 2.5 cm diameter underneath the tumor resection cavity.
4. Virtual SR-surgery was applied to the head model. The SR surgery entailed placing five burrholes of 1.5 cm diameter on the skull with the central burrhole directly above the resection cavity. We investigated five different configurations of burrholes as described in Sect. 2.5.

In our third step, the head models were created using the segmented image with virtual tumor cavity, residual tumor, and with or without burrholes. The final head mesh with each burrhole configuration consisted of a total number of approximately 4,750,000 tetrahedral elements, assigned to more than 11 types, including white matter, gray matter, CSF, scalp, skull, muscle, blood, eyeballs, tumor resection cavity, residual tumor, and burrholes.

In our fourth step, the electrode arrays were placed on the skin surface for each head model (see Fig. 7) and conductivity values were assigned to the different compartments, consisting of skin (0.25 S/m), bone (0.010 S/m), CSF (1.654 S/m), grey matter (GM) (0.276 S/m), white matter (WM) (0.126 S/m), residual tumor 0.24 S/m)

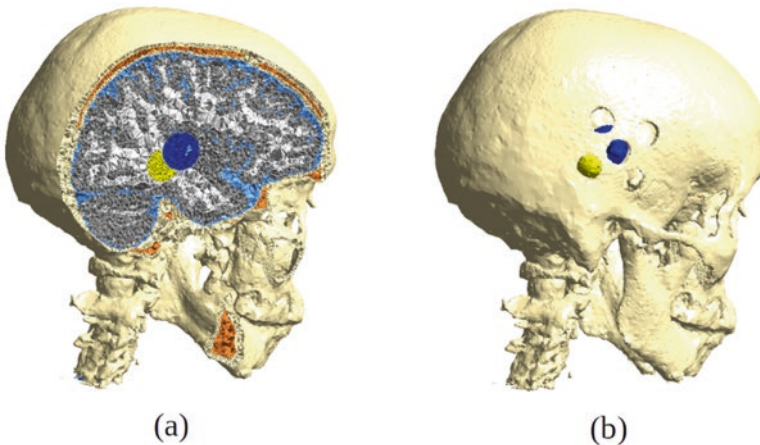


**Fig. 6** (a) The head model is based on a healthy person "Ernie" MRI and the following spherical 2.5 cm resection cavity (blue) and spherical 2.5 cm residual tumor (yellow) was manually added based on a trial patient's postoperative MRI and CT. (b) shows the five burrholes, each 1.5 cm in diameter. The central burrhole is placed directly over the resection cavity

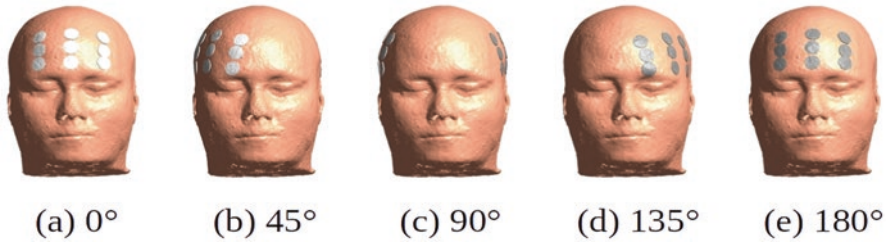


**Fig. 7** Surface reconstruction of the head model showing different electrode array positions used for simulation. Electrode arrays are comprised of 9 electrodes of 20 mm in diameter arranged in a 3×3 array pattern. The center-to-center distances between the electrodes are 45×22 mm. A 15-degree stepwise rotation of an electrode array was conducted around a central craniocaudal axis in the same horizontal plane, corresponding to degrees of 0, 15, 30, 45, 60, 75, 90, 105, 120, 135, 150, 165, and 180 for a total of 13 different positions. Figure (a)–(e) give five exemplary positions. Electrodes are paired gray with white

and necrotic tissue (1.0 S/m). We created a custom version of SimNIBS and provided scripts for automated simulation of TTFIELDS induced electric fields for variations of the electrode array positions (described in the following section).

At last, the results of the simulations were visualized using Gmsh.

## 2.4 Electrode Array Placement

Previous research indicates that SR-surgery alters the distribution of the field density in the skull and that there are electrode array positions that are the most optimal when taking into consideration the tumor- and SR-surgery positions [5, 8].

To systematically examine the optimal placement of the electrode arrays a 15-degree stepwise rotation of an electrode array was conducted around a central craniocaudal axis in the same horizontal plane, corresponding to degrees of 0, 15, 30, 45, 60, 75, 90, 105, 120, 135, 150, 165, and 180 for a total of 13 different positions as shown in Fig. 7.

FEM calculations were performed for each electrode placement with and without the chosen SR-surgery configuration.

## 2.5 SR-Surgery Location in Relation to the Tumor on the Electric Field

To test the hypothesis that the burrholes should be placed directly above the tumor resection cavity to maximize the electric field directly underneath, three additional simulations were performed. Each SR-surgery configuration was moved to three alternative positions as shown in Fig. 8. The electrode arrays were rotated as

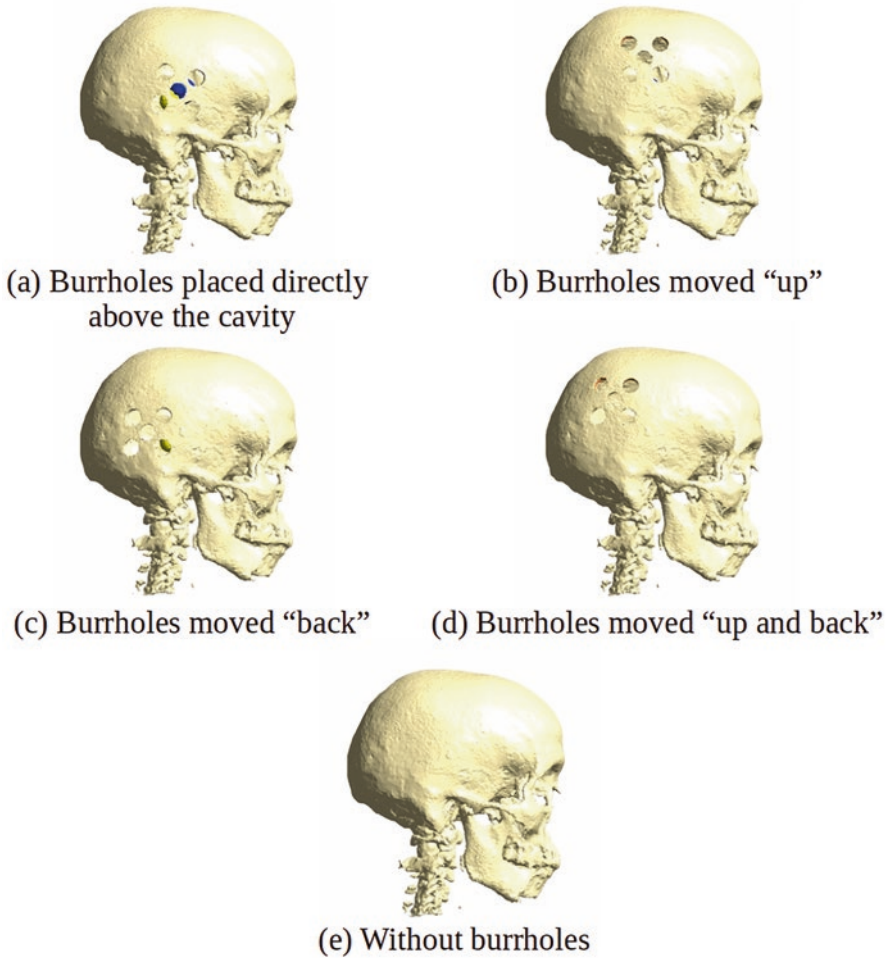


**Fig. 8** (a) Top left corner shows the original placement directly above the resection cavity. The three locations were moved 3 cm in each direction “up” (b), “back” (c), and “back and up” (d). (e) is with intact skull that serves as a control

described in Fig. 7 while the electric field was calculated. For all SR-surgery, positions electrodes array rotation overlapped the burrholes. These simulations were performed to examine if small variations in the SR-surgery location had an impact on the electric field in the resection cavity and residual tumor.

### 3 Results

1. Burrholes significantly increased the mean, median, and peak electrical field intensities in residual tumor tissue and the resection cavity (Figs. 9 and 11).
2. The effects of burrholes on the distribution of field strengths in healthy tissues were minor (Figs. 9 and 11).
3. The highest field intensities are seen in the resection cavity and residual tumor when the burrholes and electrode array are placed as close as possible above the mentioned tissue. This is illustrated when comparing mean values of the optimal electrode array placement of 60 degrees with a suboptimal placement of 150 degrees (Figs. 10 and 13).
4. The lowest electric field values in the residual tumor tissue and resection cavity were observed for positions 0 and 180 degrees (Figs. 11, 12, and 13). The mean range for those two electrode positions was for all tissues and SR-surgery positions between 77.93 – 101.96 v/m. This indicates that electrode array positions that are far away or parallel with the burrholes should not be used since the direction of the current does not pass as strongly through the region of interest, i.e., residual tumor and resection cavity.
5. Placing the burrholes directly above the resection cavity increases the field strength in the residual tumor and resection cavity by 60–80% for most electrode array positions. The highest increase in the residual tumor was observed with the burrholes located at position (d) “up and back” and electrode placement 135–150 degrees. This aligns with the burrholes and electrode array being close to directly on top over the residual tumor but not the resection cavity (Fig. 12).

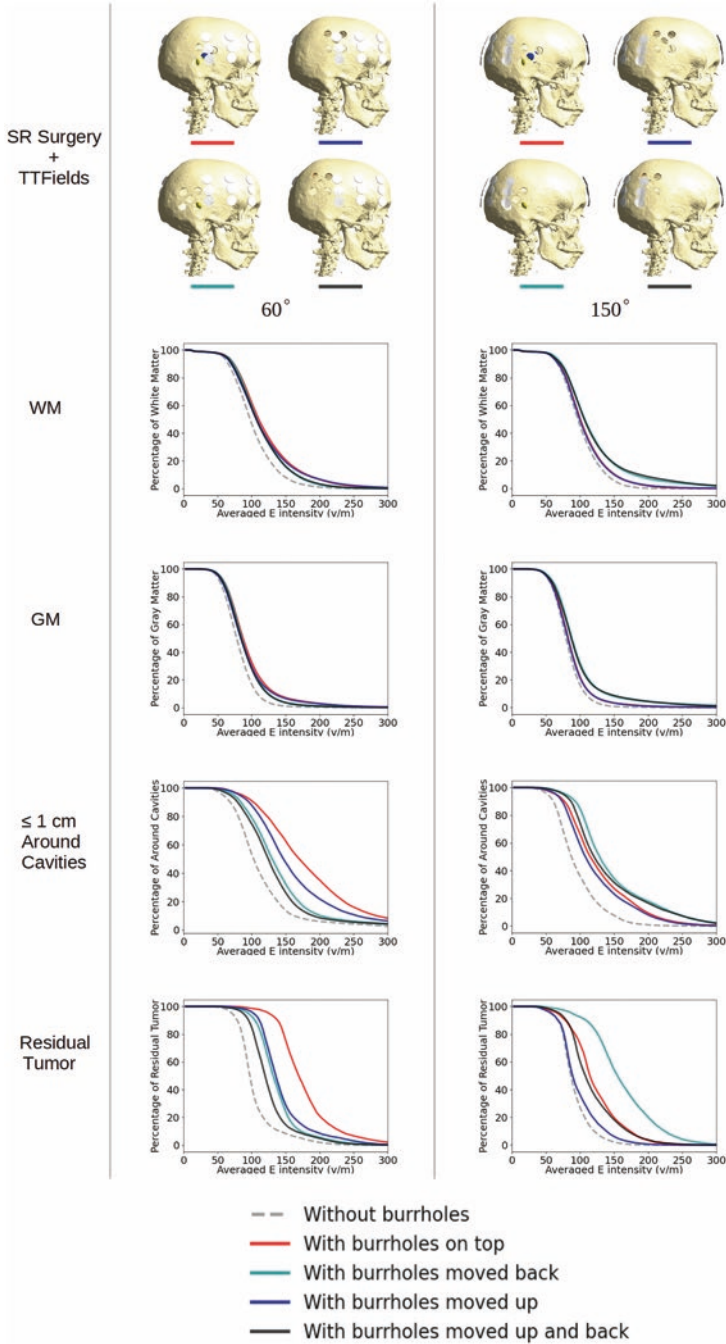
### 4 Summary and Discussion

The five burrhole SR-surgery configuration was chosen for OptimalTTF-2 trial, where the central burrhole should be placed above the center of the residual tumor/resection cavity.

After the first trial patient underwent SR-surgery, the presented realistic computational head model study was performed, mimicking the patient’s tumor resection cavity, residual tumor, and location. The exact burrhole location and size were mimicked from the postoperative CT scan of the head.

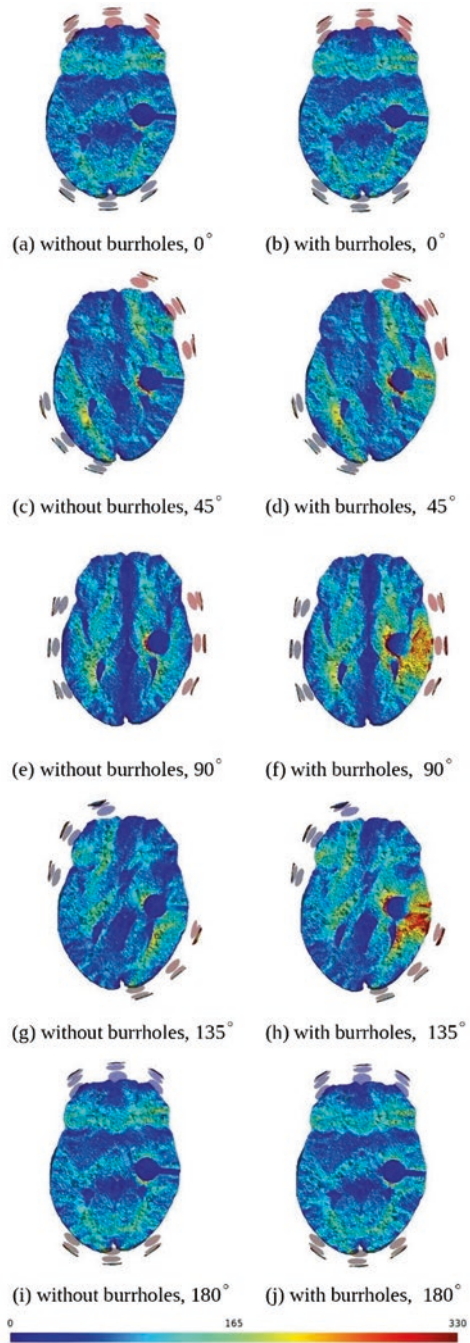
The field strength was calculated with and without SR-surgery including electrode array rotation around the craniocaudal axis. The results indicated this SR-surgery configuration significantly increases the electric field strength in the residual tumor and resection cavity when the electrodes are placed near or directly above the burrholes.

Finally, the SR-surgery configuration was moved to three alternative locations to examine if the central burrhole needed to be placed above the resection cavity as



**Fig. 9** Cumulative distributions of electrical field strengths were obtained with burrholes directly above the resection cavity (red lines), the three alternative placements as shown in Fig. 8, and without burrholes (dotted lines). The cumulative distributions in the y-axis are given as the percentages of tissue (white matter, gray matter, resection cavity, and residual tumor) exposed to field strengths above the corresponding values in the x-axis. The position of the electrode array is selected to compare the optimal 60-degree placement and suboptimal 150-degree placement

**Fig. 10** Axial view of TTFields intensity distributions in a head model that mimicked a trial patient's postoperative MRI. The approximate positions of electrodes are shown as the surrounding patches. The left and right columns give the field distributions without and with burrholes, respectively. This show the field intensity distributions induced by electrode array positions: 0°, 45°, 90°, 135°, and 180° (their corresponding electrode montages are given in Fig. 7). The field strength increases significantly when the electrodes are placed close to or directly above the burrholes



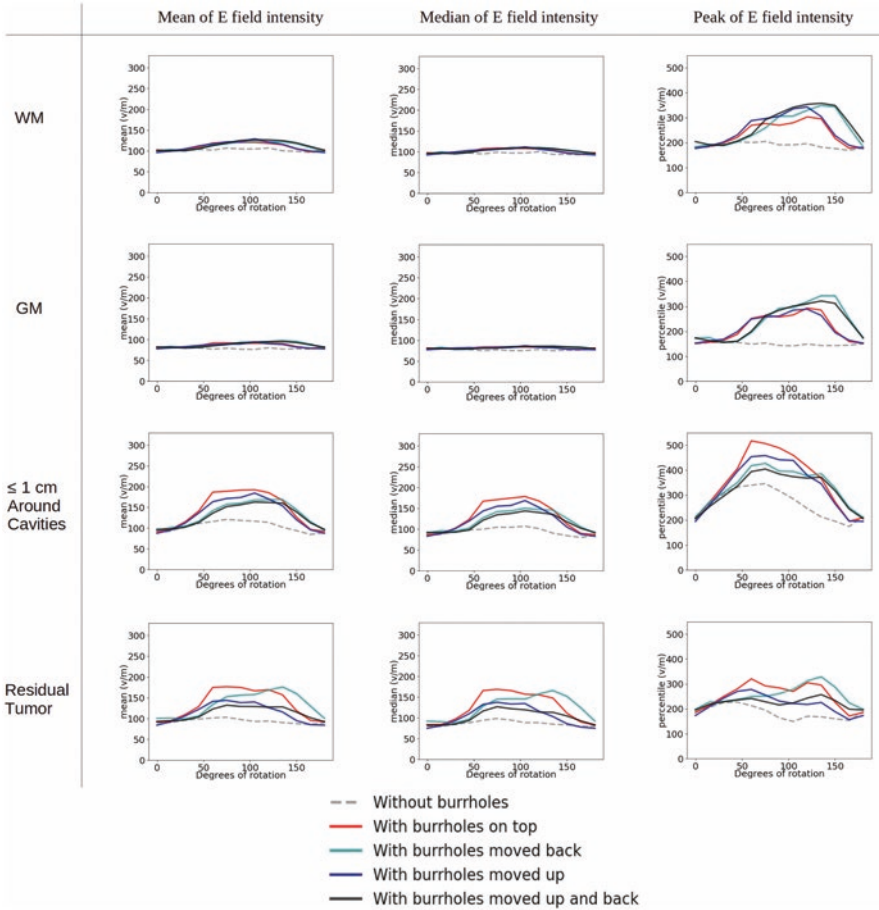


**Fig. 11** Statistical analysis of TTFields intensities with burrholes directly above the resection cavity (red lines), the three alternative positions as shown in Fig. 8 and without burrholes (dotted lines). The three columns represent the mean, median, and peak values of TTFields intensities for the four tissue types (WM, GM, residual tumor, and resection cavity). The x-axis shows the degree of rotation as seen in Fig. 7 and the y-axis shows the field strength in v/m. The peak values are defined as the 99% percentile of the field intensities. The median and peak fields follow similar patterns for each tissue. The TTFields intensities of WM and GM are similar with or without burrholes. The residual tumor and resection cavity field strength increase with burrholes, especially when they are close to or directly on top of the burrholes (corresponding to 60-150 degrees). Within this interval, the exact location of the electrodes can largely affect the peak values of the field intensities. The medians of field intensities are less sensitive to the electrodes' locations if they are set close to the burr holes

initiated planned. For each alternative location, the rotation of the electrode array placement around the craniocaudal axis was performed.

This concluded that the central burrhole and the entire SR-surgery configuration should be placed directly above the resection cavity and residual tumor since the

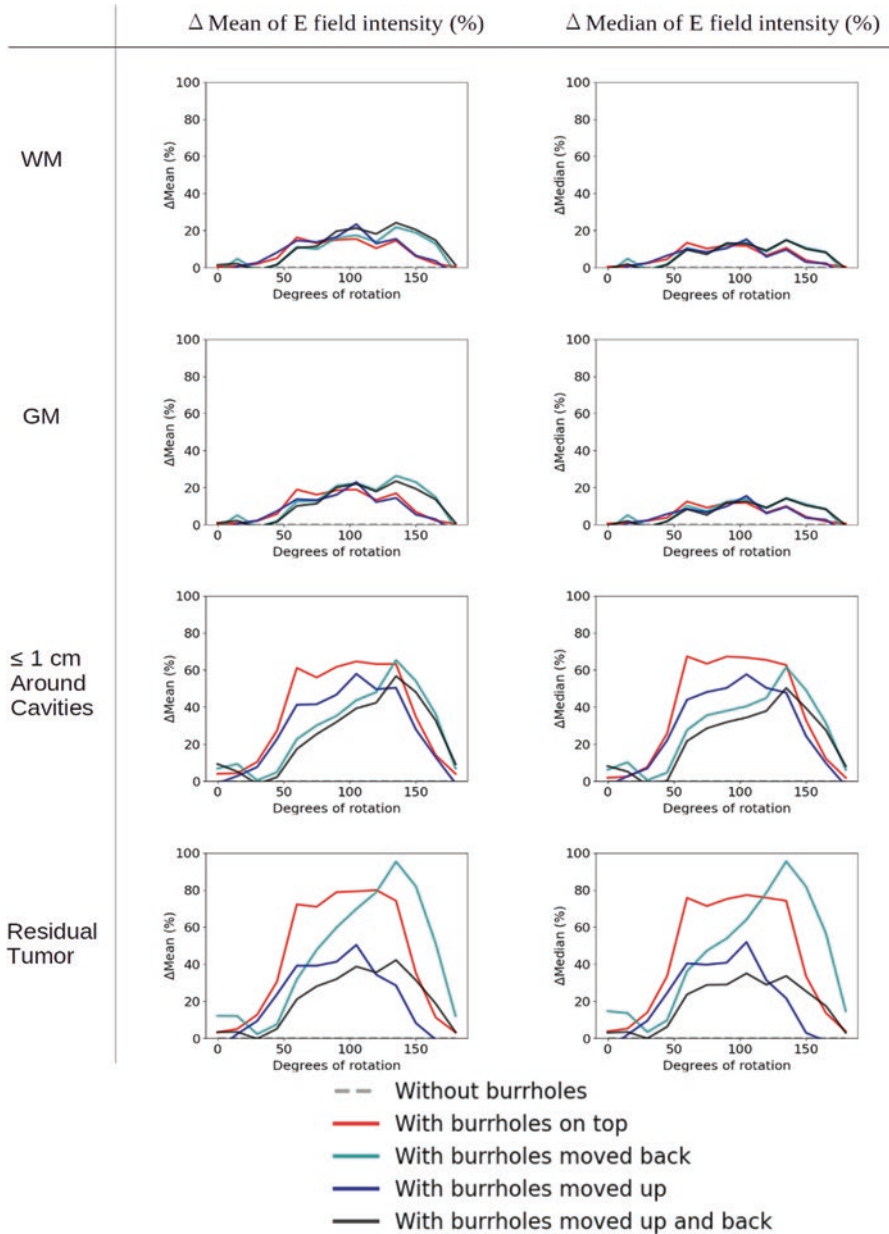


**Fig. 12** The mean and median E field intensity for WM, GM, resection cavity, and residual tumor. Without burrholes are shown as the dotted line and it can be seen at the level of the x-axis. X-axis also shows the degree of electrode array location. The y-axis represents the % increase in field intensity when SR-surgery is performed. The burrholes directly on top (red lines) and their alternative locations

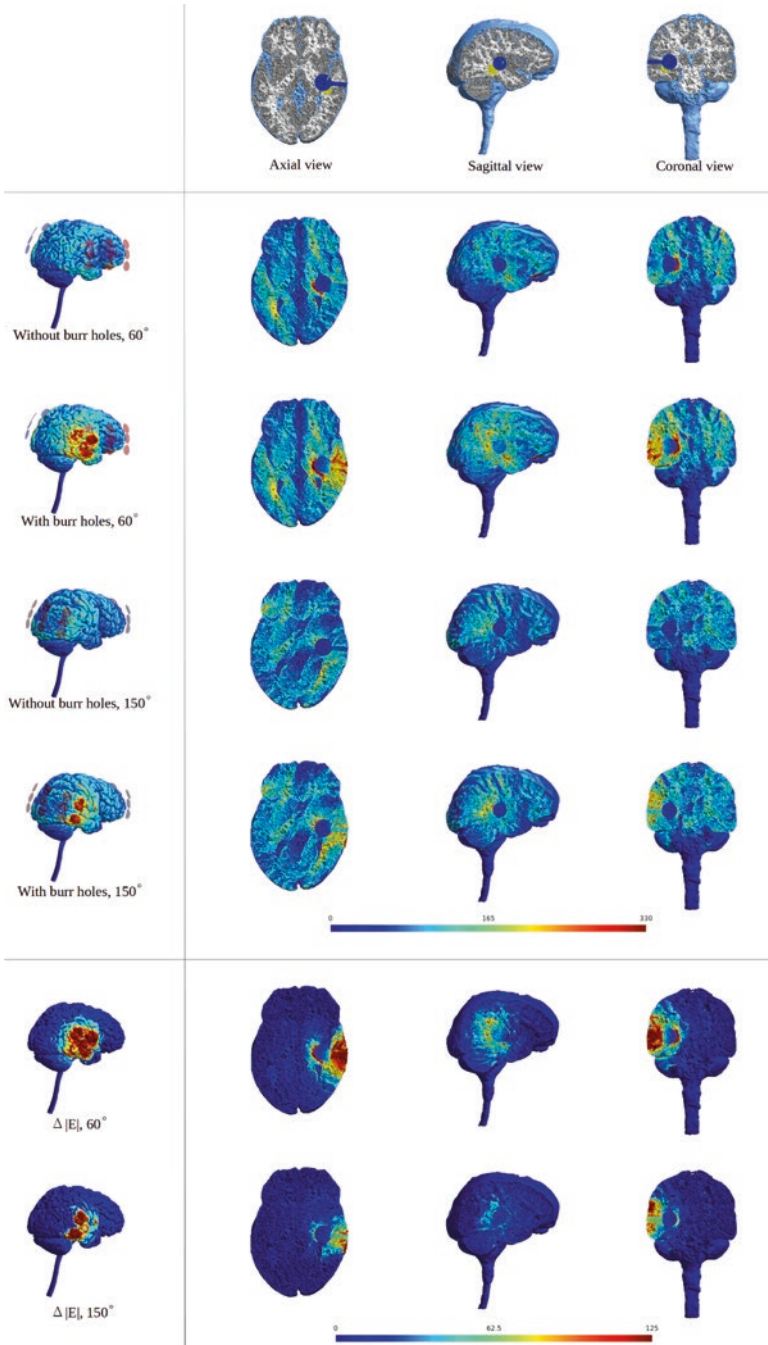


**Fig. 13** Computational head model based on a healthy MRI with manually implemented features that mimicked a real patient's postoperative MRI. Burrholes were manually added based on the

burrholes significantly increase the field strength of the pathological tissue directly underneath.

These results that SR-surgery can improve the electric field and that it is possible to optimize the electrode array placement aligns well with previous research on this topic [5, 9, 10].

These results will form the basis for the standard operating procedure for SR-surgery configuration, its location, and electrode placement for each patient individually in the OptimalTTF-2 trial.

There are a number of limitations to the work presented. This study was based on one computational head model study. The results and conclusion are therefore based on a limited amount of data that might not be valid if additional simulations were made. The residual tumor and resection cavity used in the head model might not accurately reflect the complex and heterogeneous morphology and location of all glioblastoma tumors.

The five burrhole configuration was not tested in detail. Korshøj et al. conclude that several small burrholes are more effective than one big craniectomy, however, it remains unanswered what is the optimal amount of burrholes regarding field strength and without compromising patient safety.

Furthermore, the results that the burrhole location should be placed above the pathological tissue seem intuitive. In scenarios where you only have a resection cavity or a complete tumor intact, the chose where to place the burrholes will be simple. The burrhole placement choice is more uncertain when the choice is between a large residual tumor in the far periphery of the resection cavity.

Therefore, future studies are needed to validate our findings in a larger number of heterogeneous models. We plan on examining the field strength for all the trial patients with and without SR-surgery, with realistic head modeling based on their MRI, CT, electrode placement, TTFields therapy data and compare with PFS, OS, and topographical areas of recurrence seen on the patients control MRI.

Another point worth addressing is that the burrholes conductivity values were set to be the same as CSF, which may not accurately reflect reality, in which scar tissue may also constitute a part of this volume. This could give misleading results for

---

←

**Fig. 13** (continued) postoperative CT-scan as shown in Fig. 4. The top three views (axial, sagittal) show a “funnel” or surgical access way and a resection cavity represented in blue. The tumor remnant is shown in yellow. The highest field strength was observed with electrode placement of 60 degrees. This was compared with a suboptimal electrode placement of 150-degrees. The observation is that the electric field strength is significantly enhanced in the tumor and resection cavity when electrode arrays are placed near or on the SR-surgery. **Values: 60-degree electrode array placement.** Burrholes directive above: Resection cavity 186.73 v/m, residual tumor 175.07 v/m, white matter 118.95 v/m, gray matter 91.96 v/m. Burrholes furthest away in the “back and up” position: Resection cavity 136.01 v/m, residual tumor 123.05 v/m, white matter 113.13 v/m, and gray matter 85.14 v/m. **150-degree electrode array placement.** Burrholes directly above: Resection cavity 126.49 v/m, residual tumor 118.99 v/m, white matter 105.11 v/m, and gray matter 83.25 v/m. Burrholes furthest away in the “back and up” position: Resection cavity 183.97 v/m, residual tumor 115.6 v/m, white matter 199.33 v/m, and gray matter 92.93 v/m

patients wearing TTFields therapy for months and years since their burrholes are covered in scar tissue.

More research is warranted to address several of the above-mentioned issues.

## 5 Conclusion

In this chapter, we continue to explore the novel idea of skullremodeling surgery to optimize TTFields therapy and the importance of electrode array placement. The concept of SR-surgery (craniectomy, burrholes, and skull thinning) and optimal electrode array placement were examined in a phase 1 pilot trial, OptimalTTF-1 that concluded skullremodeling surgery to be safe and indicated an increased survival for first recurrence glioblastoma.

The additional knowledge presented in this chapter is how skullremodeling surgery was attempted to be standardized to one SR-surgery configuration, its placement and electrode array placement for the entire subsequent multi-center efficacy phase 2 trial “OptimalTTF-2”.

Validating one SR-surgery configuration as the optimal would have a significant clinical impact since it would ensure uniformity of SR-surgery across the multi-center trial and thus increase the quality of the trial.

A five burrhole skullremodeling surgery was proposed and with one realistic computational head modeling calculated to have a significant increase effect on the residual tumor and resection cavity region without increasing the field strength for grey- and white matter. The realistic head model was recreated using patient-specific MRI and CT data. There was a significant increase in electric field strength when the electrodes were placed near the skullremodeling surgery. The skullremodeling surgery technical aspect was described. The location of skullremodeling surgery mattered and the most optimal location was with the central burrhole placed above the residual tumor or resection cavity. The data generated from these simulations will be used for the standard operating procedure for skullremodeling surgery and TTFields electrode array placement, however, the results are based on limited data. Therefore, more research is planned by validating this approach from all individual patient data gathered from the trial as it progresses and depending on these results the standard operating procedure should be updated accordingly.

## References

1. R. Stupp et al., Effect of tumor-treating fields plus maintenance temozolomide vs maintenance temozolomide alone on survival in patients with glioblastoma: a randomized clinical trial. *JAMA* **318**(23), 2306–2316 (2017)
2. E.D. Kirson et al., Alternating electric fields arrest cell proliferation in animal tumor models and human brain tumors. *Proc. Natl. Acad. Sci. U. S. A.* **104**(24), 10152–10157 (2007)

3. M.T. Ballo et al., Correlation of tumor treating fields dosimetry to survival outcomes in newly diagnosed glioblastoma: a large-scale numerical simulation-based analysis of data from the phase 3 EF-14 randomized trial. *Int. J. Radiat. Oncol. Biol. Phys.* **104**(5), 1106–1113 (2019)
4. A.R. Korshoej et al., Enhancing predicted efficacy of tumor treating fields therapy of glioblastoma using targeted surgical craniectomy: a computer modeling study. *PLoS One* **11**(10), e0164051 (2016)
5. A.R. Korshoej et al., Importance of electrode position for the distribution of tumor treating fields (TTFs) in a human brain. Identification of effective layouts through systematic analysis of array positions for multiple tumor locations. *PLoS One* **13**(8), e0201957 (2018)
6. A.R. Korshoej et al., OptimalTTF-1: Enhancing tumor treating fields therapy with skull remodeling surgery. A clinical phase I trial in adult recurrent glioblastoma. *Neurooncol. Adv.* **2**(1), vdaa121 (2020)
7. N. Mikic et al., Study protocol for OptimalTTF-2: enhancing tumor treating fields with skull remodeling surgery for first recurrence glioblastoma: a phase 2, multi-center, randomized, prospective, interventional trial. *BMC Cancer* **21**(1), 1010 (2021)
8. A.R. Korshoej et al., EXTH-04. Guiding principles for predicting the distribution of tumor treating fields in a human brain: a computer modeling study investigating the impact of tumor position, conductivity distribution and tissue homogeneity. *Neuro-Oncology* **19**(Suppl 6), vi73 (2017)
9. A.R. Korshoej et al., Impact of tumor position, conductivity distribution and tissue homogeneity on the distribution of tumor treating fields in a human brain: a computer modeling study. *PLoS One* **12**(6), e0179214 (2017)
10. A.R. Korshoej et al., Enhancing tumor treating fields therapy with skull-remodeling surgery. The role of finite element methods in surgery planning. *Ann. Int. Conf. IEEE Eng. Med. Biol. Soc.* **2019**, 6995–6997 (2019)

**Open Access** This chapter is licensed under the terms of the Creative Commons Attribution 4.0 International License (<http://creativecommons.org/licenses/by/4.0/>), which permits use, sharing, adaptation, distribution and reproduction in any medium or format, as long as you give appropriate credit to the original author(s) and the source, provide a link to the Creative Commons license and indicate if changes were made.

The images or other third party material in this chapter are included in the chapter's Creative Commons license, unless indicated otherwise in a credit line to the material. If material is not included in the chapter's Creative Commons license and your intended use is not permitted by statutory regulation or exceeds the permitted use, you will need to obtain permission directly from the copyright holder.

